

## СЕДИМЕНТОЛОГИЯ И СИКВЕНС-СТРАТИГРАФИЯ ВТОРОЙ НИЖНЕЙ ПАЧКИ ПАЛЕОГЕННОГО ВОЗРАСТА СВИТЫ ШАХЭЦЗЕ, БЛОК W79, НЕФТЯНОЕ МЕСТОРОЖДЕНИЕ ВЭНЬЛЮ (*бассейн Бохайского залива, Китай*)

Цзинчжэ Ли, Цзиньян Чжан, Шаша Лю, Чжунли Фан,  
Хуаньхуань Сюэ, Чжунцян Сунь, Тао Юй

Стратиграфический анализ высокого разрешения второй нижней пачки свиты Шахэцзе блока W79 бассейна Бохайского залива (Китай) показал, что область исследования, ранее рассматриваемая как мелководная дельтовая система, в действительности возникла преимущественно в субаэральной обстановке, в которой были выявлены осадочные системы распределенных флювиальных комплексов (РФК). На основе региональной корреляции литофаций в различных осадочных системах создана стратиграфическая модель высокого разрешения, включающая 2 продолжительных цикла базового уровня, 6 умеренно продолжительных циклов базового уровня и более 58 кратковременных циклов базового уровня. Сиквенс-граница SB1 маркирует верхнюю часть целевого интервала и представляет мощный непрерывный слой аргиллитов, перекрывающих обогащенные песком отложения канала. Сиквенс-граница SB2 маркирует основание целевого интервала и представляет слой стабильно распределенных сланцев между обогащенными песком осадками. Колебания базового уровня включают существенную тектоническую составляющую, согласующуюся с региональной тектонической обстановкой. Во время активной стадии погружения в осадочных толщах зафиксированы полциклы поднятия базового уровня, а во время относительно стабильной стадии - полциклы опускания базового уровня.

*Распределительный флювиальный комплекс, нефтяное месторождение Вэньлю, блок W79, свита Шахэцзе, сиквенс-стратиграфия, седиментология*

## SEDIMENTOLOGY AND SEQUENCE STRATIGRAPHY OF THE PALEOGENE LOWER SECOND MEMBER OF THE SHAHEJIE FORMATION, W79 BLOCK, WENLIU OILFIELD, BOHAI BAY BASIN, CHINA

Jingzhe Li<sup>1</sup>, Jinliang Zhang<sup>1,2</sup>, Shasha Liu<sup>1</sup>, Zhongli Fan<sup>2</sup>, Huanhuan Xue<sup>2</sup>, Zhongqiang Sun<sup>2</sup>, and Tao Yu<sup>2</sup>

<sup>1</sup>College of Resources Science & Technology, Beijing Normal University, Beijing 100875, China

<sup>2</sup>College of Geological Science and Engineering, Shandong University of Science and Technology, Qingdao 266500, Shandong, China

High-resolution stratigraphic analysis of the lower second member of the Shahejie Formation of the W79 Block of Bohai Bay Basin, China, has revealed that the study area, previously interpreted as a shallow water delta system, actually originated mainly in a subaerial setting with a distributive pattern. Depositional systems of the distributive fluvial complex (DFC) have been recognized. The regional correlation of the lithofacies within the different depositional systems has led to a high-resolution-stratigraphic framework of two long-term base level cycles, six middle-term base level cycles, and more than 58 short-term base level cycles. Sequence boundary SB1 marks the top of the target interval and is characterized by thick and continuous mudstone overlying sand-rich channel sediments. Sequence boundary SB2 marks the bottom of the target interval and is characterized by stably distributed shales between sand-rich sediments. The base-level fluctuation has a strong tectonic component consistent with the regional tectonic setting; during the active subsidence stage, base-level rising semi-cycles were recorded in the strata, and during the relatively stable stage, base-level falling semi-cycles were recorded.

*Distributive fluvial complex; Wenliu Oilfield; W79 Block; Shahejie Formation; Sequence stratigraphy; Sedimentology*

### 1. INTRODUCTION

Originating from seismic stratigraphy, sequence stratigraphy has absorbed newly found results from conventional stratigraphy, sedimentology and other disciplines and has become a new branch of geology (Mitchum et al., 1985; Galloway, 1989; Miall, 1991; Posamentier and James, 1993; Cross et al., 1993; Catuneanu, 2002). Conventional sequence stratigraphy has been effectively used in marine environments, whereas in continental environments, it faces many limitations (Deng et al., 2002). With the development of the oil industry, increasing attention has been given to fluvial stratigraphy, and thus many theories have been modified or adapted to continental environments (Schumm, 1993; Shanley and McCabe, 1993, 1994; Currie, 1997; Martinsen et al.,

© Jingzhe Li<sup>1</sup>, Jinliang Zhang<sup>✉</sup>, Shasha Liu<sup>1</sup>, Zhongli Fan, Huanhuan Xue, Zhongqiang Sun, Tao Yu, 2016

✉ e-mail: jinliang@bnu.edu.cn

DOI: 10.15372/GiG20160607

1999; Blum and Törnqvist, 2000; Holbrook and Bhattacharya, 2012). High-resolution sequence stratigraphy, originally conceptualized by the genetic stratigraphy research group of the Colorado School of Mines, is one of the techniques that could effectively solve the problems faced in continental exploration and development (Cross et al., 1993). Using A/S (accommodation/ sediment supply) analysis and base level cyclic correlation, high-resolution sequence stratigraphy provides a new method to accurately describe reservoirs on a small layer scale (Deng et al., 2002).

The W79 Block, one of the most important blocks of the Wenliu Oilfield, has already entered the middle to late stage of the developing period. The Paleogene lower second member of the Shahejie Formation ( $Es_2^L$ , lowermost Oligocene succession, ranging from approximately 2700 m to 3000 m) of this block, originally described as a shallow water delta system deposit, is the main oil-bearing interval of this area (the oil-bearing area is nearly 13.4 km<sup>2</sup>) and has plentiful remaining petroleum resources. However, because of its complicated sedimentary features, many studies (Fu et al., 2005; Li and Peng, 2007; Fu, 2008; Wang 2011; Hu et al., 2014) concerning sequence stratigraphy and sedimentary facies models have remaining controversies, which restrict the further development of this block. Hence, this paper aims to provide an analysis of the sequence stratigraphic and sedimentary characteristics of the  $Es_2^L$ , Paleogene Shahejie Formation of the W79 Block based on abundant well-logging data, 3D seismic data and core data under the principles of high-resolution sequence stratigraphy and sedimentology.

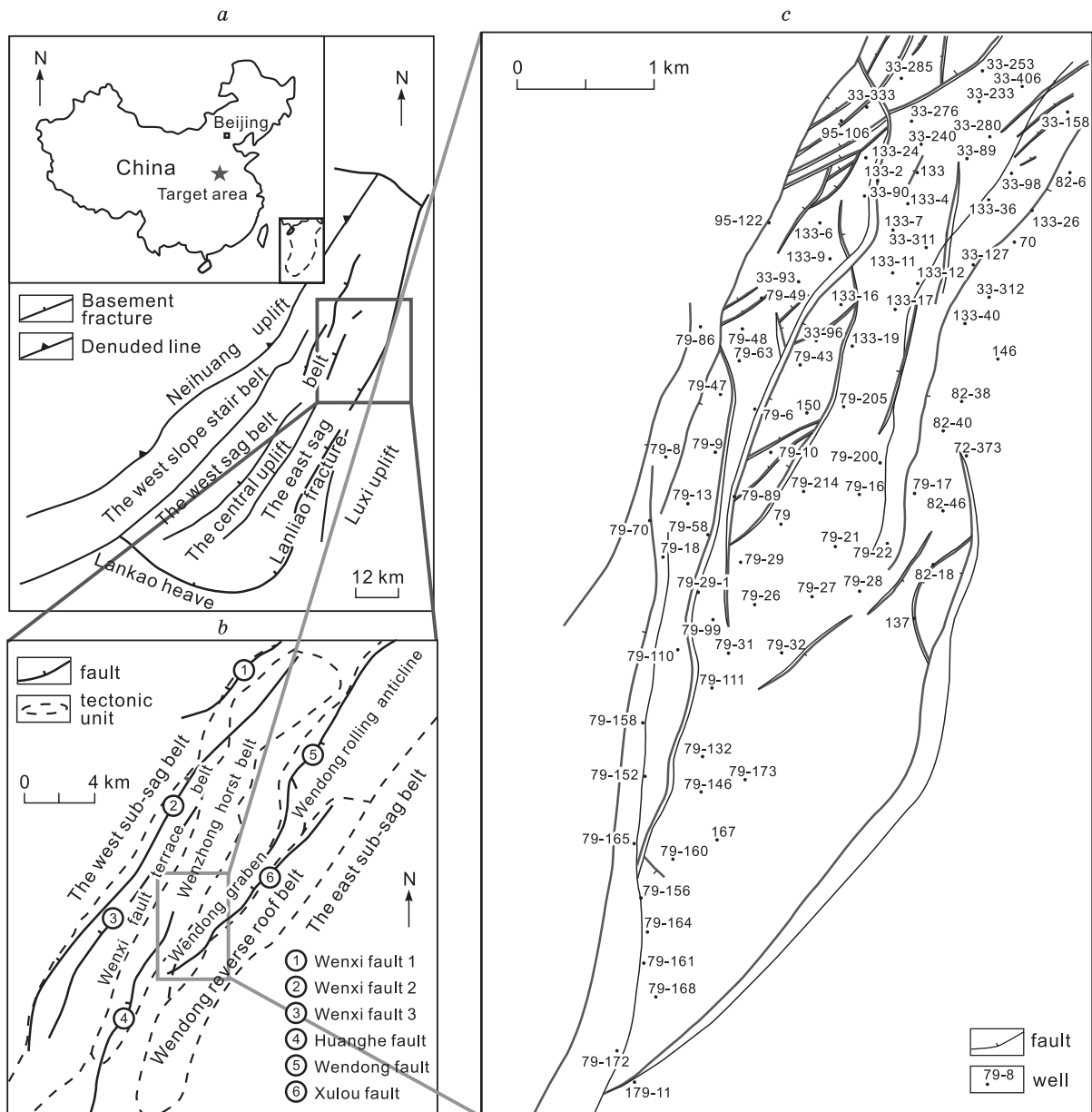
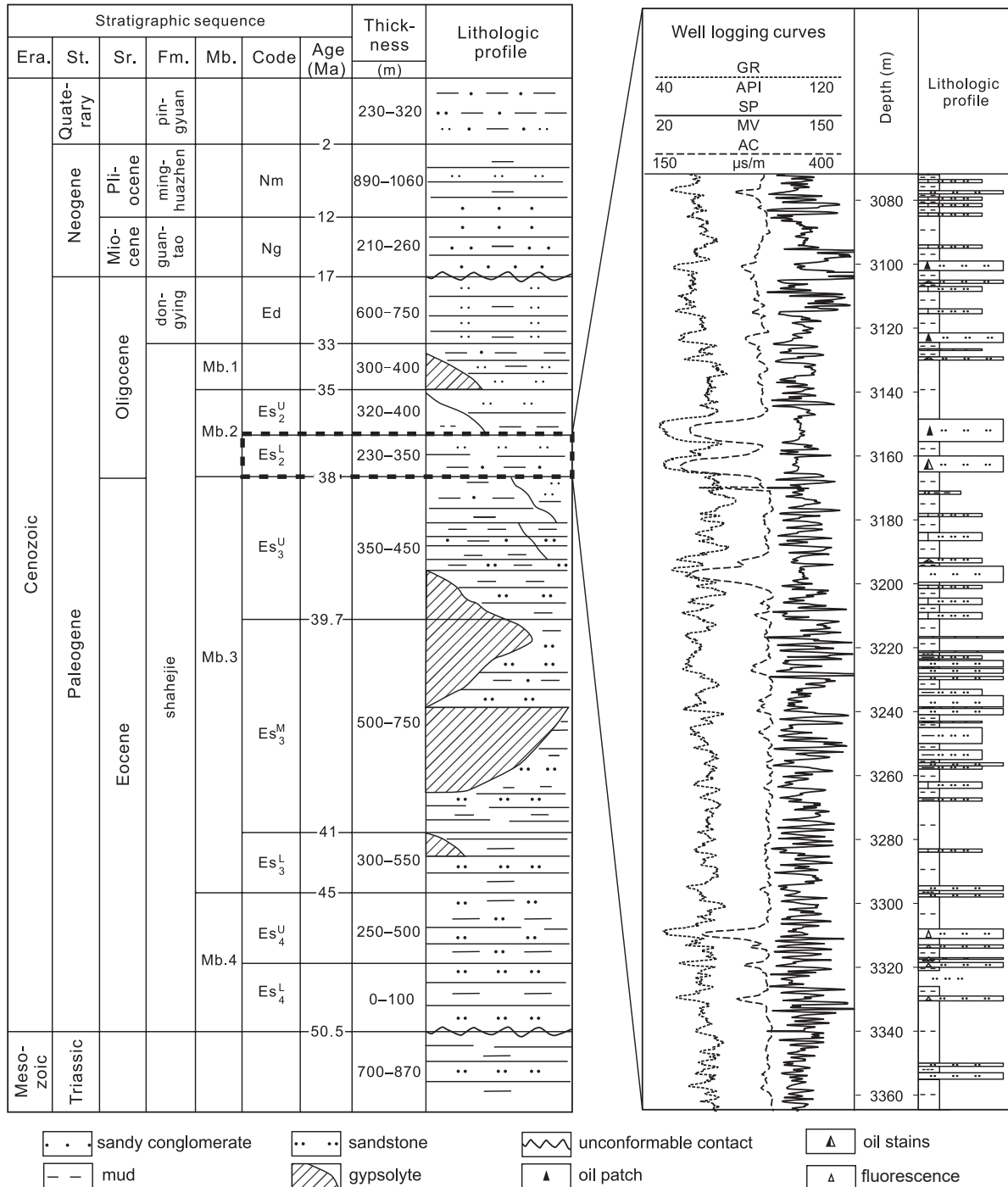


Fig. 1. Location of W79 Block showing the main structures and well points

## 2. REGIONAL GEOLOGY AND STRATIGRAPHY

The Dongpu Depression, located in the south margin of Bohai Bay Basin is an oil-rich sedimentary depression. It is a 16-km long and 70-km wide NNE fault depression that covers an area of approximately 5300 km<sup>2</sup> (Fig. 1a). The Dongpu Depression formed from the Huabei Movement in the late Paleogene. The evolution of the depression reveals an evident tectonic component and shows periodic features (Dai, 2012). It is bounded by the Luxi Uplift in the east, the Lankao Uplift in the south and the Neihuang Uplift in the west. Its northern margin is the Maling Fault, which is also the southern margin of the Linqing Depression. The Lanling, Changyuan and Huanghe basement rift faults controlled the early evolution of the Dongpu Depression and



**Fig. 2. Stratigraphy in Dongpu Depression, Bohai Bay Basin (the left), enhancing the lower second member of Shahejie FM. in Well W167 of W79 Block (the right). St. System; Sr. Series; Fm. Formation; Mb. Member.**

changed it from a broom fault depression to a double-break fault depression. During the early Paleogene, the Tan-Lu Faults changed from transpression to dextral lateral strike-slip faults, altering the regional stress field from a shear-extrusion field to a shear-tensile field. Differential subsidence also occurred during this period. The regional shear-tensile effects caused the Central Uplift rise, then induced gravitational sliding and salt rock intrusion, and finally molded the present appearance of the Dongpu Depression (Wang, 2011; Dai, 2012).

The Wenliu Oilfield, located in Henan Province, is situated on the northern part of the central uplift of the Dongpu Depression. Bounded by two large sag belts (i.e., the West and the East Sub-sag Belt), the Wenliu Oilfield is a complicated fault zone that is characterized by alternately distributed horsts and grabens (Fan et al., 1995). It is also of the NNE direction and is approximately 20 km long and 16 km wide, covering an area of more than 2000 km<sup>2</sup> (Fig. 1b).

The W79 Block, the target area of this study and a large block in the southern part of the Wenliu Oilfield, is located in a graben bounded by two large faults (i.e., the Wendong Fault and Xulou Fault) and is a NNE fault-lithological reservoir. Most faults in the block are normal faults. These faults can be classified into two groups: one group is characterized by a NNE direction and the other is characterized by a NE direction (Fig. 1c). The W79 Block is approximately 20 km<sup>2</sup>. It is located next to the Wen82 Block in the east, the Wen95 Block in the west, the Wen43 Block in the north and the Wen179 West Block in the south.

The stratigraphy of this fault depression mainly contains, from bottom up, Mesozoic, Paleogene Shahejie Formation, Dongying Formation, Neogene Guantao Formation, Minghuazhen Formation and Quaternary Pingyuan Formation. The Shahejie Formation can be divided into Four Members (from bottom up is 4th member, 3rd member, 2nd member and 1st member). The 2nd member can further be divided into lower and upper parts (Fig. 2). The lower part of the 2nd member, namely the target interval, discussed in this paper, is not quite sand-rich, but has very good porosity and permeability. The overlying upper part of the 2nd member consists of a steadily distributed argillaceous rock or argillaceous rock with gypsum, and could serve as a set of good cap rock (Hao, 2012).

### 3. MATERIALS AND METHODS

The W79 Block is characterized by abundant available materials, including a 3D seismic database (covering an area of about 35 km<sup>2</sup>), more than 340 drilling wells and logging data (including core data of over 330 m from 8 cored wells of the area), and plentiful analysis test data. Thus, it is possible to launch a detailed sequence stratigraphic study.

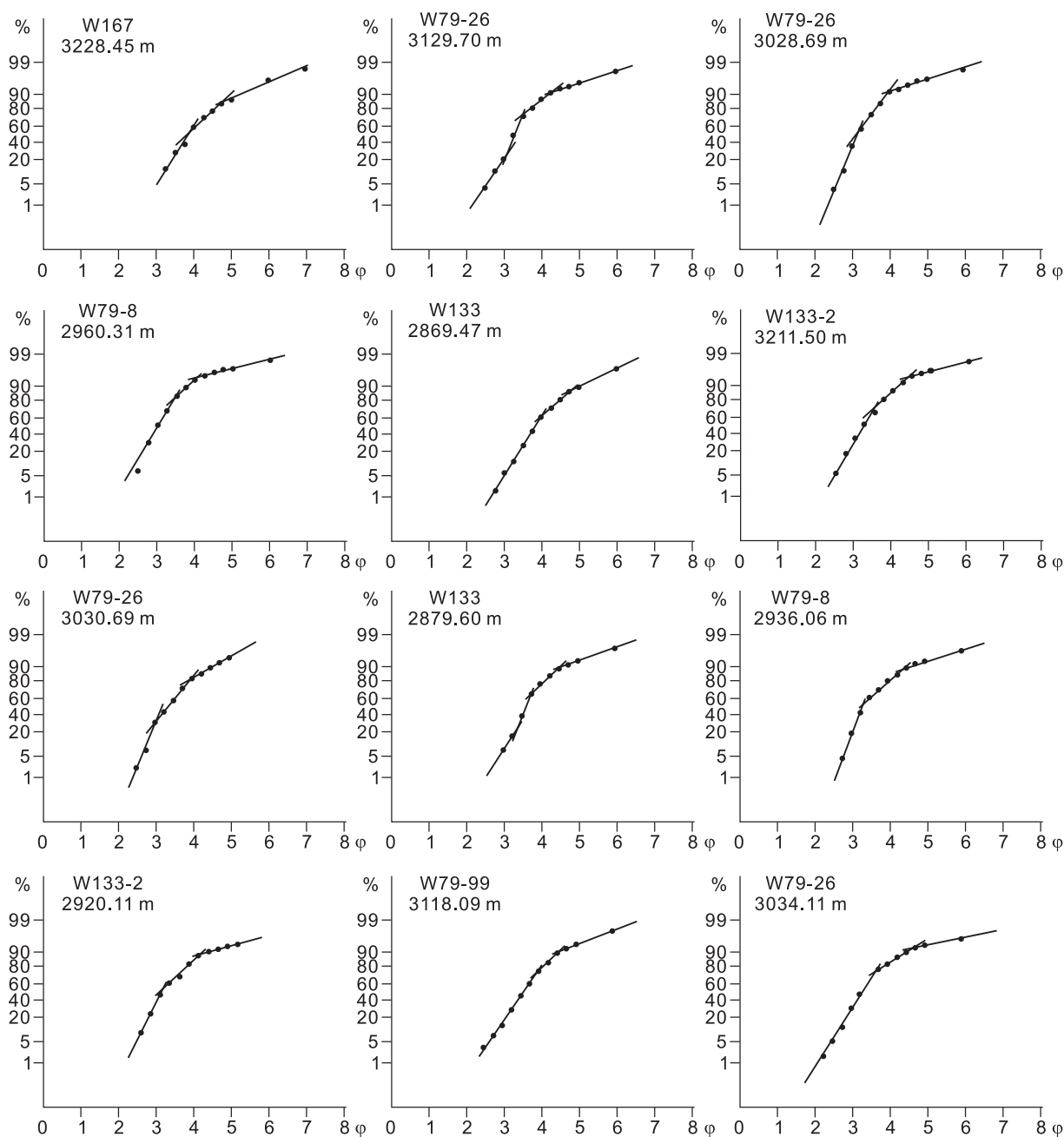
First, an integrated well-seismic correlation was made. With the 3D seismic database, regional reflection surfaces were traced to the target area. Using a synthetic seismogram and several VSP logging data, the relationships between the seismic and well data were established, and key seismic surfaces were recognized on the corresponding well logs (especially the bottom and top surface of the target interval). According to the structural features of the target area, more than ten seismic-well sections were interpreted and the exact positions of the fault points on the wells were identified. Then, a more precise sequence stratigraphic study was performed, mainly using the well data. Wavelet transformation and Maximum Entropy Spectral (MEM) analysis of Gamma Ray curves were also used to extract hidden cyclical characteristics of stratigraphic sequences and to identify the major depositional tendencies for describing the geological characteristics of the target interval.

Simultaneously, lithological and facies analyses were conducted. One of the first steps in the facies analysis of a clastic reservoir is the description and interpretation of available conventional cores. Tens cores were taken from the target interval of the W79 block, and all of the cores were described, focusing on the sediment color, sedimentary structures and visual grain size. Grain-size analysis was performed on the core samples collected from all 7 cored wells with a LS130 Coulter laser micro-granulometer. The heavy mineral combination was also counted. The ratio of stable transparent heavy minerals (mainly zircon and tourmaline) to the entire transparent heavy minerals (zircon, tourmaline, garnet, epidote, etc.) was conducted to verify the sedimentary sources. Based on the core descriptions and the subsequent laboratory tests, the associations of sedimentary structures, sediment grain size and some other sedimentary features were classified. According to the specific pack of these associations, the sedimentary facies were interpreted. Finally, based on the detailed stratigraphic framework and counted sand body data, the lithofacies paleogeographic characteristics were analyzed, and along with the interpreted types of facies, a depositional model was established and the possible distribution of sedimentary facies were predicted both laterally and vertically.

### 4. SEDIMENTARY MODEL

#### 4.1 Lithofacies characteristics

The reservoir properties of sedimentary rocks depend on a series of allogenic and autogenic processes (e.g., tectonism, eustasy, sediment influx biological processes, climate, etc.). At the basin scale, these processes interact to



**Fig. 3. Grain size cumulative probability plots of target interval in Wenliu Oilfield**

produce depositional system tracts of different stratigraphic architectures over time (Miall, 1985). At smaller scales, these processes determine the colors, shapes, structures, textures and internal properties of clastic sedimentary bodies. It is at this smaller scale that the lithological characteristic analysis and lithofacies recognition becomes of great significance in the reservoir depiction.

The core description along with well logging data analysis shows that the main lithology of the target area mainly includes mudstone, sandy mudstone, siltstone, muddy siltstone, limy siltstone, and sandstone. The main color of sandstone is light brown, whereas the main color of mudstone is red to purple. Statistics shows that mudstone is the dominant lithology of the target interval (more than 63%), with the other components showing relatively smaller percentages (siltstone 14.5%, muddy siltstone 5%, limy siltstone 5% and sandstone 12.5%). Shapes of grain-size cumulative curves plotted on log-probability paper could reveal environmental characteristics (Visher, 1969; Sagoe and Visher, 1977). The plots of grain size as cumulative curves of the target interval show that suspension population occupies a large proportion (generally larger than 30%). Saltation population is dominant and its segment is relatively steep. The truncation points between these two populations are usually bigger than 3( $\phi$  value).



**Fig. 4. Contour lines of the heavy mineral assemblage proportion of the target interval**

Traction population is usually missing within the target interval (Fig. 3).

The ratio of stable transparent heavy mineral assemblage (mainly zircon and tourmaline) to the entire transparent heavy mineral amount (zircon, tourmaline, garnet, epidote, etc.) is around 75% in the northwestern part, while it is about 80% in the central part. As the share of garnet quickly decreases (the main changing component is actually the garnet, because the amount of epidote is very rare and its variation could be ignored), the ratio rises to 85%. The ratio of this terrigenous-mineral assemblage shows an overall increasing trend from northwest to southeast. Since the anti-weathering ability of garnet is relatively weaker than those of zircon and tourmaline, the higher ratio reveals the longer transportation distance. The paleocurrents might be southeastward. Thus, the source lands are supposed to be on the NNW direction (Fig. 4).

In addition to the lithological function, the more important result of the core description is the subdivision of cores into lithofacies. The categorization is based on lithology, grain size, physical and biogenic sedimentary structures, and stratification, which reveal the depositional processes that produced them. Lithofacies and lithofacies associations (groups of related lithofacies) are the basic units for the interpretation of depositional environments (Holz et al., 2000; Zhang and Xie, 2008; Vakulenko et al., 2010; Srivastava, 2013; Eltom, 2014). Seventeen lithofacies have been recognized within the study interval, ranging from fine-grained sandstones of parallel bedding to mudstones of lenticular structures (Fig. 5). The codes, features and interpretation are summarized in Tab. 1.

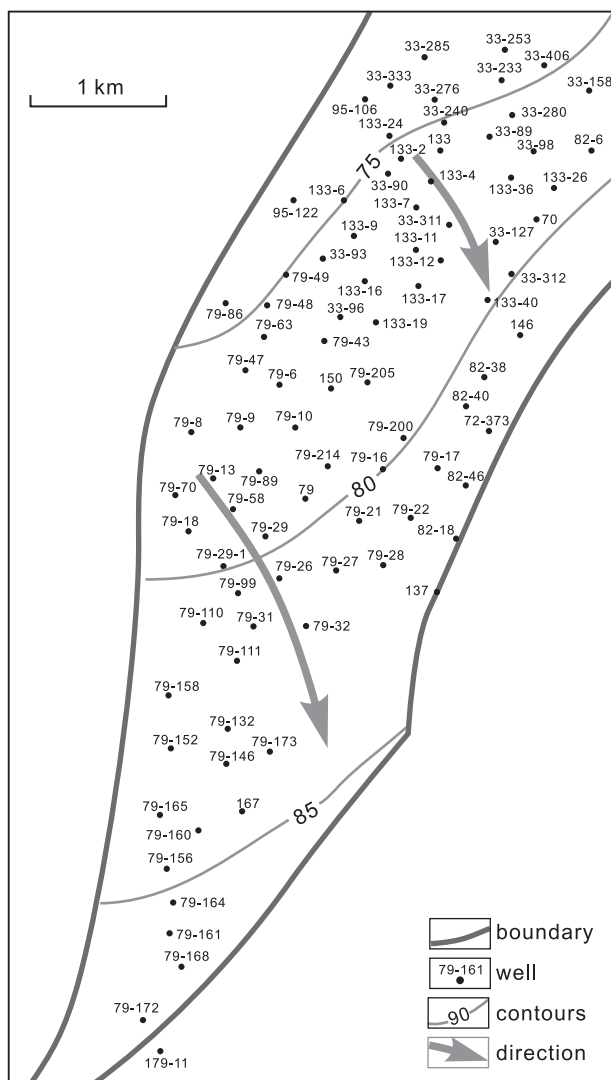
According to the reddish brown mud of subaerial oxidizing features and the grain size cumulative plots revealing typical channel deposit features (Fig. 3), along with the specific associations of the lithofacies as reconstructed from the core descriptions, a Distributive fluvial complex is interpreted to be responsible for the sedimentation.

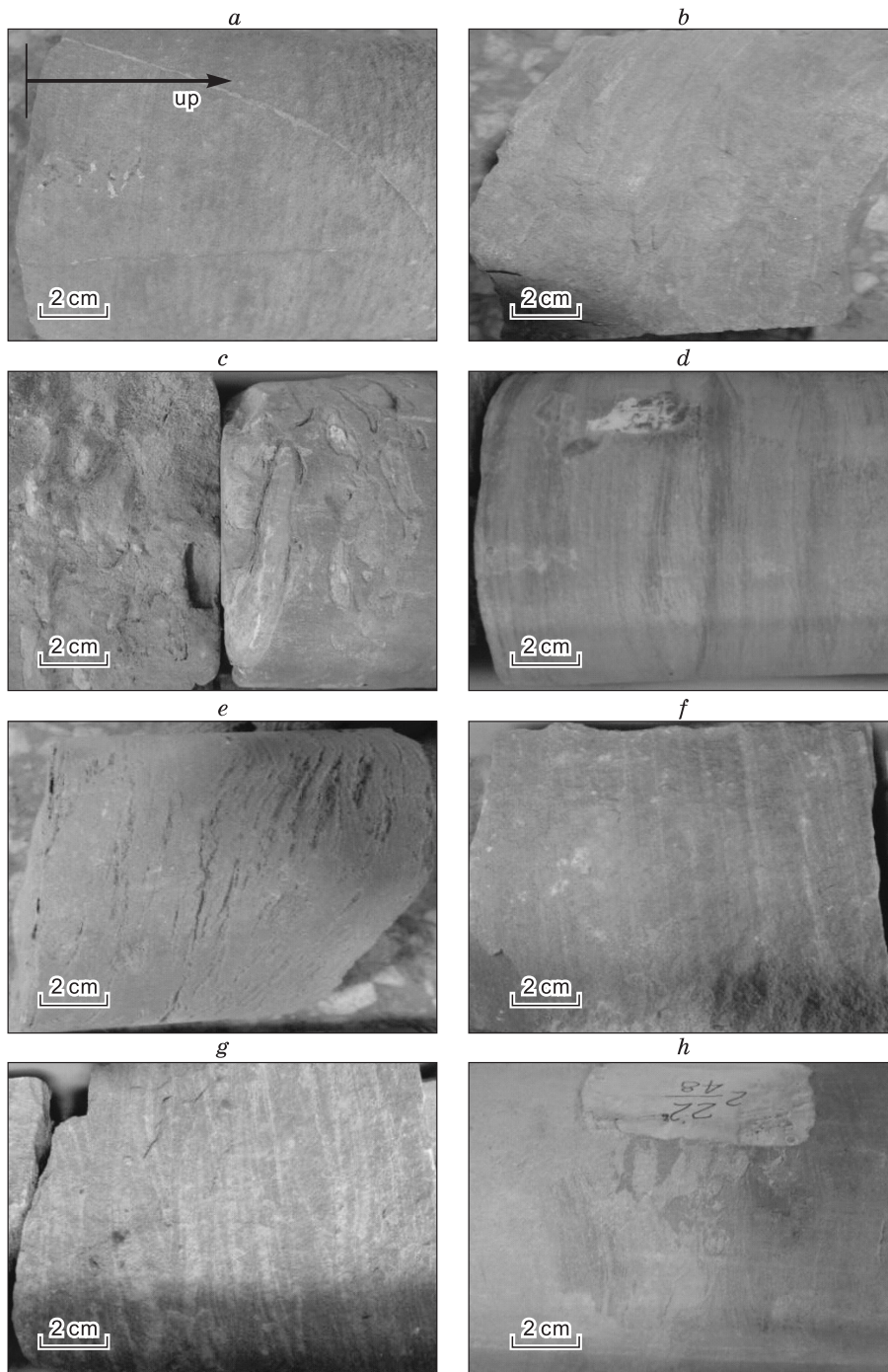
#### 4.2 Distributive fluvial complex (DFC)

The target interval of the Dongpu Depression was formed in a rift contraction basin environment far from the source and with an abundant sediment supply. Single well core section shows that channel and overbank deposits are two main sequence types of the sedimentary strata. The channel deposits generally have complete sequences and are relatively isolated. The overbank deposits are mainly composed of reddish brown Mm that could indicate the exposed and oxidic environment (together with the lack of subaqueous paleontological fossils, it may be revealed as subaerial sedimentary environment) (Fig. 6). Lithofacies paleogeographic mapping shows many meandering channels distributed along the basin margin like a large fan-shaped river system, which shows distributive characteristics quite different of those of a fan delta system (Fig. 7).

This special depositional system is interpreted to be a DFC, mainly composed of 3 subfacies (i.e., channel fill subfacies, overbank subfacies and river flood lake subfacies) (Fig. 7). In the study area, back-stepping and forward-stepping types both exist, revealing  $A/S > 1$  and  $A/S < 1$ , respectively, and their logging curve (gamma ray) reflections are generally of toothed boxes or bell shapes.

The channel fill subfacies are mainly composed of sand-rich channel deposition. From bottom to top, Ss, St, Sla, and Sr constitute the main lithofacies and show a fining-upward cycle. The grain size is relatively coarse, and the



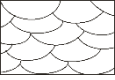

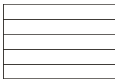

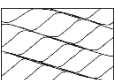

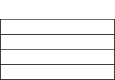

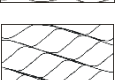
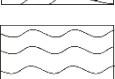
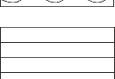

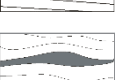

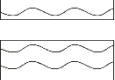
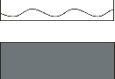



**Fig. 5. Typical lithofacies of the W79 block for the target interval: (a) Parallel bedding sandstone; (b) Trough cross-bedding sandstone; (c) Scouring structured sandstone with mud gravels; (d) Ripple cross-bedding siltstone; (e) Wavy cross-bedding siltstone; (f) Parallel bedding siltstone; (g) Ripple cross-bedding muddy siltstone; (h) Flasher structured mudstone**

**Typical lithofacies of the W79 block for the target interval: (a) Parallel bedding sandstone; (b) Trough cross-bedding sandstone; (c) Scouring structured sandstone with mud gravels; (d) Ripple cross-bedding siltstone; (e) Wavy cross-bedding siltstone; (f) Parallel bedding siltstone; (g) Ripple cross-bedding muddy siltstone; (h) Flasher structured mudstone**

Table 1.

Lithofacies of the target interval succession

ID	Lithology	Structure and texture	Interpretation	Schematic representation
<b>St</b>	sandstone	trough cross bedding	Channel lower part, curved bounding surfaces, originates by migration of 3-D bedforms, high-energy	
<b>Sla</b>	sandstone	low-angle cross bedding	Low-angle foreset lamina of single direction (generally lower than 10°), high energy	
<b>Sp</b>	sandstone	parallel bedding	Parallel and acclinic, stable and high energy	
<b>Ss</b>	sandstone	Scouring	Channel bottom, erosional bounding surface, usually mingled with mud gravels, high-energy	
<b>SSr</b>	siltstone	ripple cross-bedding	Superimposition of one ripple on another as the ripples migrate, abundant sediment supply (especially suspension population)	
<b>SSla</b>	siltstone	low-angle cross bedding	Low-angle foreset lamina of single direction (generally lower than 10°)	
<b>SSp</b>	siltstone	parallel bedding	Parallel and acclinic, result of suspension settling of fine-size sediment	
<b>SSt</b>	siltstone	trough cross bedding	Curved bounding surfaces, originates by migration of 3-D bedforms	
<b>MSSr</b>	muddy siltstone	ripple cross-bedding	Superimposition of one ripple on another as the ripples migrate, abundant suspension sediment supply	
<b>MSSw</b>	muddy siltstone	wavy bedding	Wavy lamina, parallel to the bounding surface as a whole, abundant sediment supply of clay and silt	
<b>MSSp</b>	muddy siltstone	parallel bedding	Parallel and acclinic, result of suspension settling of fine-size sediment or precipitation from solution, low energy	
<b>MSSla</b>	muddy siltstone	low-angle cross bedding	Low-angle bounding surfaces, originates by migration of planar bedforms, low-energy	
<b>SMf</b>	silty mudstone	flaser bedding	Fluctuating depositional conditions marked by periods of current activity, mud < sand	
<b>SMw</b>	silty mudstone	wavy bedding	Wavy lamina, parallel to the bounding surface as a whole, abundant sediment supply of clay and silt	
<b>Mw</b>	mudstone	wavy bedding	Wavy lamina, parallel to the bounding surface as a whole, abundant sediment supply of clay	
<b>Mm</b>	mudstone	massive bedding	Contain few or no visible internal lamina, overbank or abandoned channel deposits	
<b>MI</b>	mudstone	lenticular bedding	Fluctuating depositional conditions marked by periods of current activity, mud > sand	



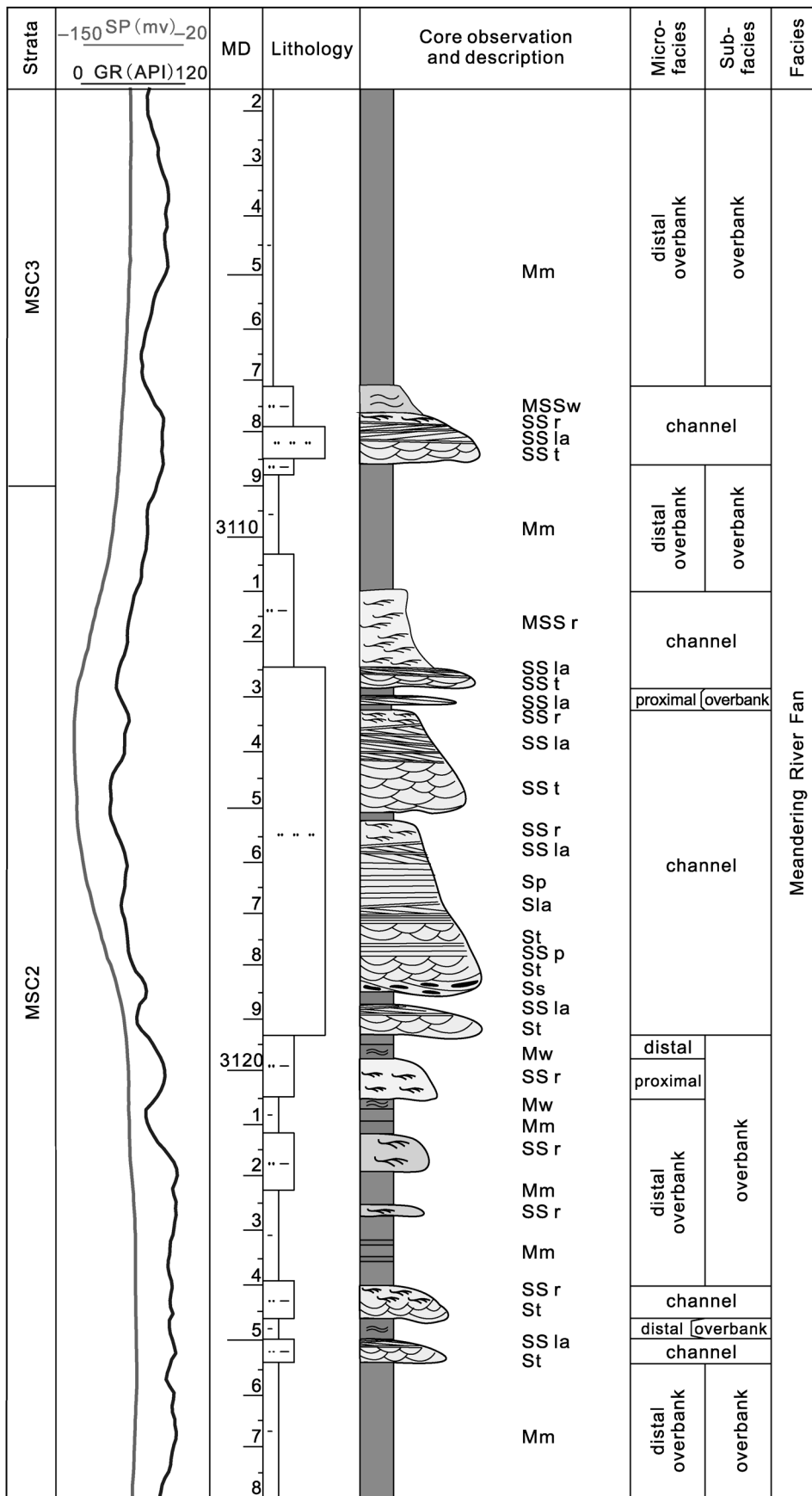


Fig. 6. Single well facies (W133-12 Well)

Table 2.

Comparison of DFC and shallow water delta

	DFC	Shallow water delta
<b>Settings</b>	Mainly subaerial	Subaqueous and subaerial
<b>Paleo-climate</b>	Humid; Oxidizing environment (major part) to slightly reductive environment (some small parts)	Relatively humid; Reductive environment to slightly oxidizing environment
<b>Subaqueous paleontological fossils</b>	Rare	Relatively abundant
<b>Wave or tide forces</b>	No	Yes
<b>Sediment supply</b>	Sufficient	Sufficient
<b>Deposits between distributive/distributary channels</b>	Mud	Mud or sand sheet
<b>Distance between distributive/distributary channels</b>	Relatively large	Small to medium
<b>Sequence and cyclicity</b>	Mainly positive cycles	Both positive and negative cycles
<b>Subfacies</b>	Channel fill subfacies, overbank subfacies and river flood lake subfacies	Delta plain subfacies, delta front subfacies, and pro-delta subfacies

sandbody connectivity is therefore high. The overbank subfacies contain two parts. The proximal overbank is next to the channel and is one of the most important reservoir types due to its good physical properties (i.e., after channel fill). The common lithofacies of the proximal overbank include Sla, SSla, and SSr. The distal overbank is distributed between channels and is mainly composed of purple to red mudstone. The common lithofacies include MSSw, SMw, and Mm. The river flood lake subfacies form near the distal overbank, recording stand water, and are mainly composed of greyish-green mudstone. The common lithofacies of this subfacies contain Mw, Mm, and Ml.

## 5. SEQUENCE STRATIGRAPHY

### 5.1 Sequence Stratigraphic Surfaces

The identification of sequence stratigraphic surfaces and classification of depositional trends is the core component of high resolution stratigraphic correlation and division. Integrated seismic and well analyses shows that two major sequence stratigraphic surfaces collaboratively limit the target interval:

SB1, the top surface of the target interval, has strong and continuous reflection in the seismic section (Fig. 8a). It is a regional parallel unconformity and is characterized by overlying thick and continuous shale of Es<sub>2</sub><sup>U</sup>. Its features on the well logging curves are high GR (Gamma Ray), AC/DT (Acoustic) and SP (Spontane-

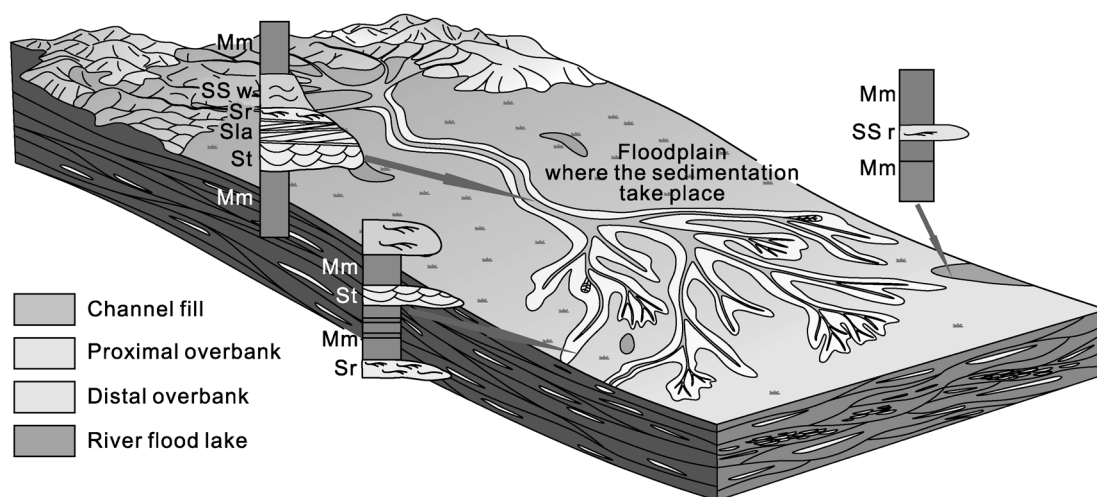


Fig. 7. Sedimentary facies model of the target interval in Dongpu Depression

ous Potential) values and a low R25 (2.5 m Resistivity) value. Below this surface, tooth shaped AC/DT and GR curves become the main characteristics, revealing a frequent sand mud inter-bedding (Fig. 8b1).

SB2, the bottom surface of the target interval, also has strong and continuous reflection in the seismic section (Fig. 8a). It is also a parallel unconformity characterized by a stable mudstone layer of the underlying Es<sub>3</sub><sup>U</sup>. Its features on well logging curves are high GR, AC, SP and R25 values (Fig. 2). The most obvious characteristic is the coarsening-upward sandbody in the SP curve, approximately 10 m above the surface, in which the curve has a v-shaped low value zone (Fig. 8b2).

### 5.2 Facies Associations under Sequence Stratigraphic Frame

Based on core observations as well as integrated seismic and well analyses, more than 58 short-term base level cycles could be recognized in the target interval of the W79 Block. Genetic sequence stacking patterns can be used to define genetic sequence sets, showing base level rises and falls (Bourquin et al. 1995). Thus, these short-term patterns could be combined into 6 middle-term base level cycles (from bottom to top—MSC1 and MSC6). In a similar way, given the regional setting, these 6 middle-term base level cycles could be further

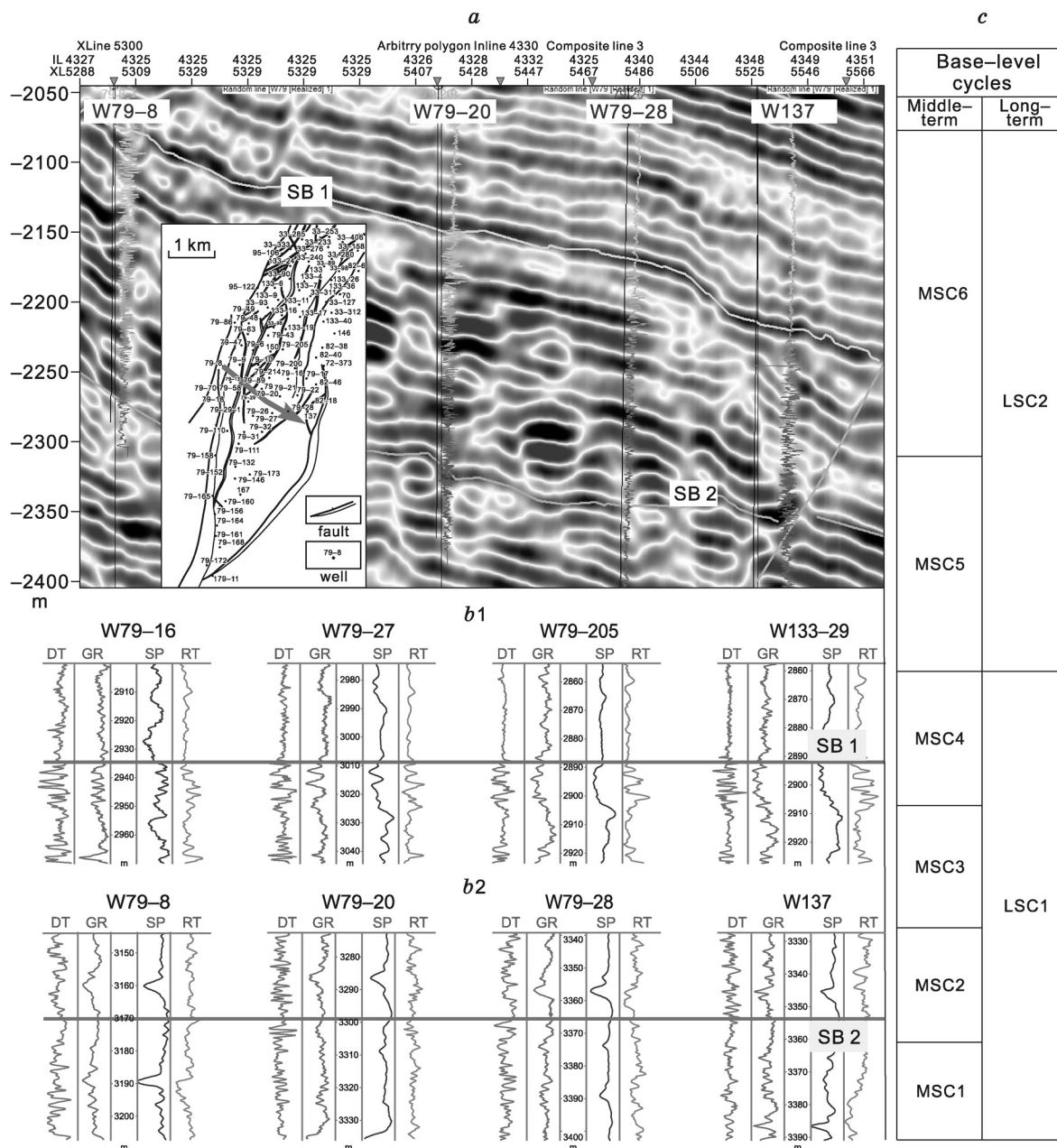
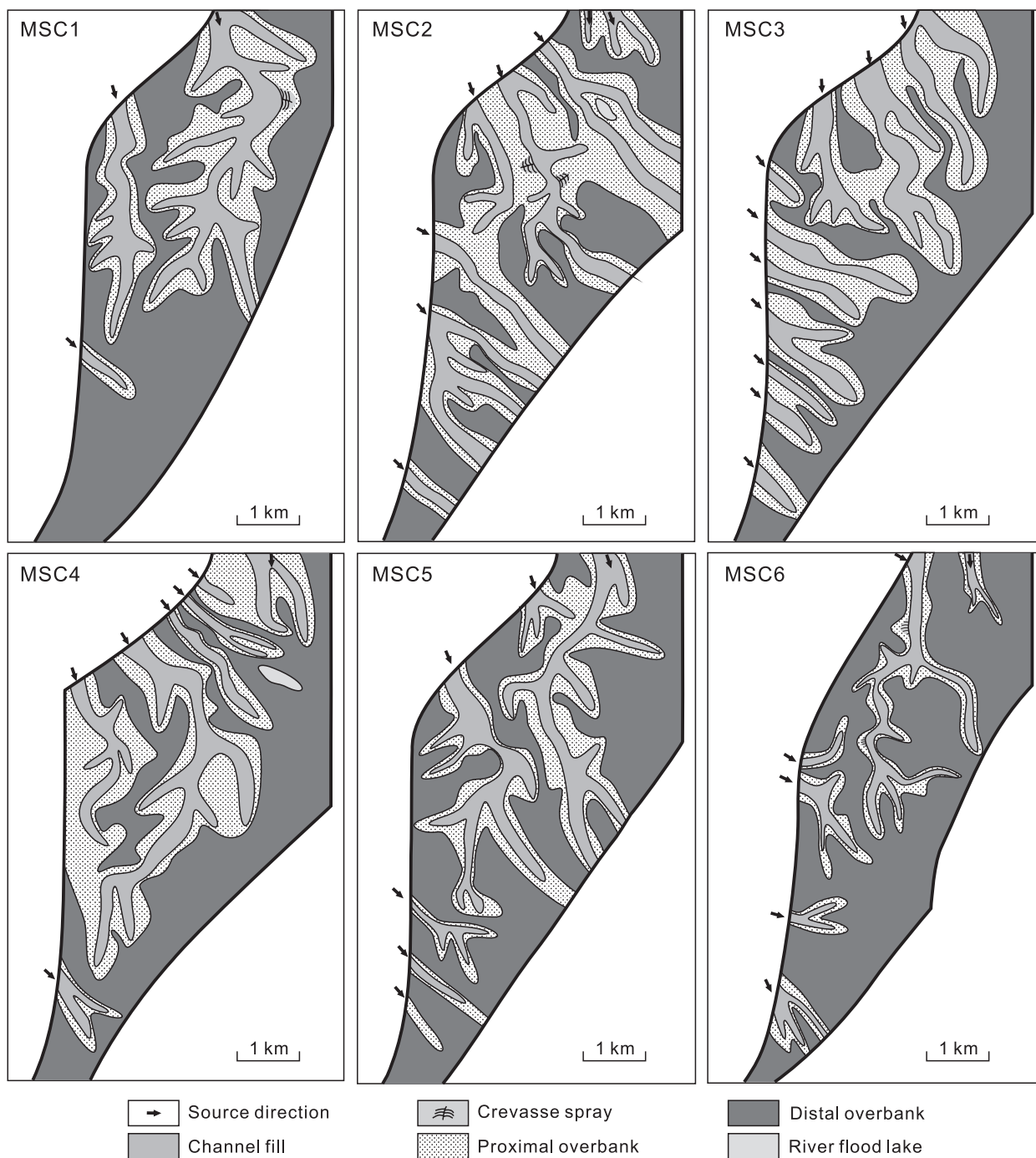


Fig. 8. Identification of main sequence stratigraphic surfaces and stratigraphic division framework



**Fig. 9. Sedimentary facies maps of the middle-term base level cycles of the target interval of W79 Block**

combined into 2 long-term base level cycles (from bottom to top—LSC1 and LSC2) (Fig. 8c). Under this high resolution sequence stratigraphic frame, according to the practice of oilfield development, a 58-small-layer plan was accepted for paleogeographic mapping (Fig. 9) and for other subsequent studies. Precise paleogeographic mapping shows that the vertical facies distribution and association have strong regulations on the long-term base level cyclic scale (Fig. 10):

LSC1, the first long-term base level cycle, composed of MSC1 to MSC4, approximately 90 m to 120 m long, is the lower part of the target interval and is limited by the SB2 at the bottom. At the lower part of this long-term base level cycle, proximal overbank deposition and distal overbank deposition are most commonly found, whereas channel fill deposition could sporadically be found. In contrast, at the upper part of this long-term base level cycle, apart from proximal and distal overbank, channel fill deposition is also commonly found



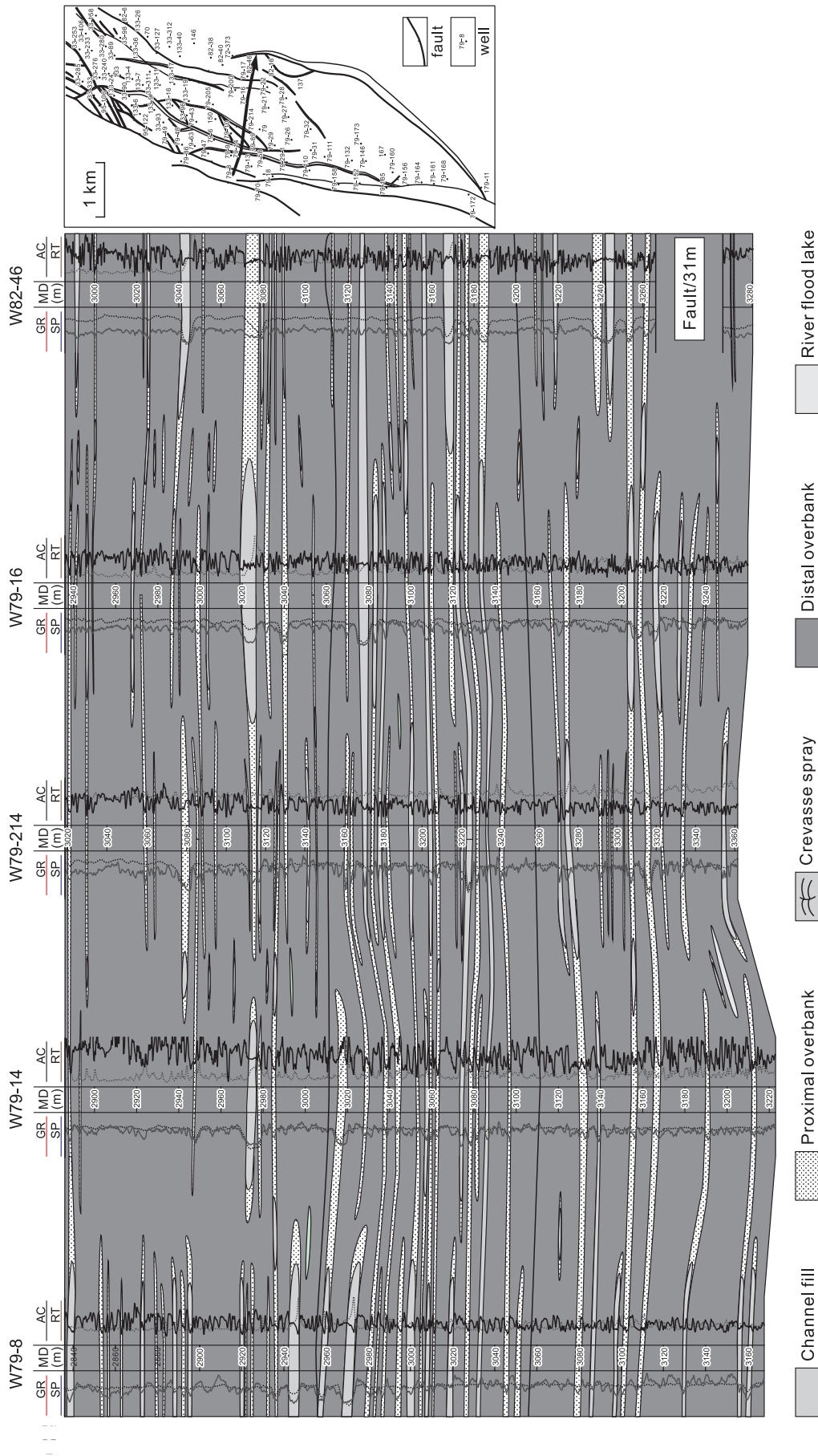


Fig. 10. Correlation section of the target interval of W79 Block, showing changes of the sedimentary facies



and the connectivity of the sandbody is relatively higher than that of the lower part of LSC1, which has no or isolated channel fill deposition. The ratio of channel fill to overbank increases from bottom to top, and the sedimentary stratigraphy shows an overall coarsening-upward trend (Fig. 10), revealing that the environment varied from a relatively higher accommodation condition to a relatively lower accommodation condition. This vertical change indicates that the entire LSC1 was formed during base level falling or an A/S decreasing period and is, in fact, a semi-cycle of the long-term scale. The vertical characteristic of LSC1 might reveal a relatively stable tectonic setting where subsidence tends to be slow and the depositional process is stable with abundant sediment supply.

LSC2, the second long-term base level cycle, composed of MSC5 to MSC6, approximately 150 m to 190 m long, is the upper part of the target interval and is limited by SB1 at the top. In the lower part of this long-term base level cycle, similar to that of the upper part of LSC1, channel fill deposition is commonly found apart from the proximal and distal overbank deposition, and the connectivity of the sandbody is relatively high. In contrast, in the upper part of this long-term base level cycle, proximal overbank deposition and distal overbank deposition are most commonly found, whereas channel fill deposition is sporadically found (Fig. 10). The sedimentary stratigraphy shows an overall upward-fining trend, revealing that the environment varied from a relatively lower accommodation condition to a relatively higher accommodation condition. Similar to LSC1, the entire LSC2 was also a semi-cycle of the long-term scale, whereas it was formed during a base level rising or A/S increasing period. The vertical characteristics of LSC2 might reveal an active tectonic setting where subsidence tends to be fast and the base level rises rapidly, which makes the ratio of the channel to overbank change from high to low.

## CONCLUSIONS

SB1 marks the top of the target interval and is characterized by thick and continuous mudstone overlying sand rich fluvial sediments. SB2 marks the bottom of the target interval and is characterized by stably distributed shale between sand-rich fluvial sediments.

The regional correlation of the lithofacies within the different depositional systems led to a high-resolution-stratigraphic framework of 2 long-term base level cycles, 6 middle-term base level cycles and more than 58 short-term base level cycles.

The base-level fluctuation shows strong tectonic and climate components consistent with the regional tectonic settings; during the active subsidence stage, base level rising semi-cycles were recorded in the strata, and during the relatively stable stage, base level falling semi-cycles were recorded.

## ACKNOWLEDGMENTS

Financial support was provided by the Fundamental Research Funds for the Central Universities. The authors acknowledge the editors and anonymous reviewers for their helpful and constructive editing and reviewing work. The authors also acknowledge permission by SINOPEC Zhongyuan Oilfield Company to publish this paper. Jingzhe Li also thanks China Scholarship Council for the financial support overseas.

## REFERENCES

- Blum M.D., Törnqvist T.E.** Fluvial responses to climate and sea-level change: a review and look forward // *Sedimentology*, 2000, v. 47 (s1), p. 2—49.
- Bourquin S., Friedenber R., Guillocheau F.** Depositional sequences in the Triassic series of the Paris basin: geodynamic implications // *J. Iberian Geol.* 1995, v. 19, p. 337—362.
- Catuneanu O.** sequence stratigraphy of clastic systems: concepts, merits, and pitfalls // *J Afr. Earth Sci.*, 2002, v. 35 (1), 1—43.
- Catuneanu O.** Principles of sequence stratigraphy // Amsterdam—Boston—Heidelberg, Elsevier, 2006, 375 pp.
- Cross T.A., Baker M.R., Chapin M.A., Clark M.S., Gardner M.H., Hanson M.S., Lessenger M.A., Little L.D., McDonough K.J., Sonnenfeld M.D., Valasek D.W., Williams M.R., Witter D.N.** Applications of high-resolution sequence stratigraphy to reservoir analysis // *Collection Colloques et Seminaires—Institut Francais du Petrole*, 1993, v. 51, p. 11-11.
- Currie B.S.** Sequence stratigraphy of nonmarine Jurassic–Cretaceous rocks, central Cordilleran foreland basin system. *Geol. Soc. Am. Bull.*, 1997, 109 (9), p. 1206—1222.
- Dai Y.** Study of the high-resolution sequence stratigraphy and sedimentary microfacies in Ming 1 fault block of Wenming Village oilfield [D] // Ocean University of China, 2012, Qingdao.

**Deng H., Wang H., Zhu Y., Cross T.A.** High-resolution sequence stratigraphy: Principle and application // Beijing, Geology Press, 2002, 398 pp.

**Fan S., Wang X., Su Y.** The fault system and structure framework in Dongpu depression and its petroleum accumulation // Fault-Block Oil & Gas Field, 1995, v. 3, 004.

**Fu J.** Paleogeographic background and sedimentary facies study on the lower of the third member of the Shahejie Formation of Paleogene in Dongpu sag // Beijing, China University of Geosciences, 2008.

**Fu M., Li W., Jia R., Su A.** Study of progressive exploration and development in Wenliu oilfield // Special Oil & Gas Reservoirs, 2005, v. 3, 003.

**Galloway W.E.** Genetic stratigraphic sequences in basin analysis I: architecture and genesis of flooding-surface bounded depositional units // AAPG Bull., 1989, v. 73 (2), p. 125—142.

**Hao J.** Studies on the mechanism and mode of deep oil and gas accumulation in Wenliu area of Dongpu Depression. MS thesis // China University of Petroleum (East China), 2012.

**Holbrook J.M., Bhattacharya J.P.** Reappraisal of the sequence boundary in time and space: Case and considerations for an SU (subaerial unconformity) that is not a sediment bypass surface, a time barrier, or an unconformity // Earth-Sci. Rev., 2012, v. 113 (3), 271—302.

**Holz M., Vieira P. E., Kalkreuth W.** The Early Permian coal-bearing succession of the Paran6 Basin in southernmost Brazil: depositional model and sequence stratigraphy // Brazilian J. Geol., 2000, v. 30 (3), p. 424—426.

**H M., Shi J., Xu J, Lu S., Huang K., Wang J.** Sedimentary model and microfacies division of Wenliu Area // Inner Mongolia Science Technology and Economics, 2014, v. 08, p. 64+67.

**Li H., Peng S.** Study on sedimentary microfacies during the middle-late development stages of Wen 72 block in Wenliu Oilfield // J. Jilin University, 2007, v. 04, p. 710—716.

**Martinsen O.J., Ryseth A.L.F., Helland-Hansen W., Flesche H., Torkildsen G., Idil S.** Stratigraphic base level and fluvial architecture: Ericson Sandstone (Campanian), Rock Springs Uplift, SW Wyoming, USA // Sedimentology, 1999, v. 46 (2), p. 235—263.

**Miall A.D.** Architectural-element analysis: a new method of facies analysis applied to fluvial deposits // Earth-Sci. Rev., 1985, v. 22 (4), p. 261—308.

**Miall A.D.** Stratigraphic sequences and their chronostratigraphic correlation // J. Sediment. Res., 1991, v. 61 (4), p. 497—505.

**Mitchum Jr R.M.** Seismic stratigraphic expression of submarine fans // AAPG Mem., 1985, v. 39, p. 117—136

**Posamentier H.W., James D.P.** An overview of sequence-stratigraphic concepts: uses and abuses // Sequence Stratigraphy and Facies Associations. Oxford, Blackwell, 1993, p. 3—18.

**Sagoe K.M.O., Visher G.S.** Population breaks in grain-size distributions of sand—a theoretical model // J. Sediment. Petrol., 1977, v. 47 (1), p. 285—310.

**Shanley K.W., McCabe P.J.** Perspectives on the sequence stratigraphy of continental strata // AAPG Bull., 1994, v. 78 (4), p. 544—568.

**Shanley K.W., McCabe P.J.** Alluvial architecture in a sequence stratigraphic framework: a case history from the Upper Cretaceous of southern Utah, USA // The geological modelling of hydrocarbon reservoirs and outcrop analogues / Eds. S.S. Flint and I.D. Bryant. Int. Assoc. Sediment. Spec. Publ., 1993, v. 15. Oxford, Blackwell, p. 21—56.

**Srivastava A.K., Mankar R.S.** Lithofacies architecture and depositional environment of Late Cretaceous Lameta Formation, central India // Arabian J. Geosci., 2015, v. 8, p. 207—226.

**Vakulenko L.G., Aksenova T.P., Yeltsov I.S., Zamirailova A.G., Yan P.A.** A lithofacies description of Jurassic sediments in the south of the Predyenisei petroleum subprovince, West Siberia // Russian Geology and Geophysics (Geologiya i Geofizika), 2010, v. 51 (4), p. 329—338 (425—436).

**Visher G.S.** Grain size distributions and depositional processes // J. Sediment. Res., 1969, v. 39 (3), p. 1074—1106.

**Wang S.** Fine reservoir description of block Wen25 in Wenliu oilfield [D] // Ocean University of China, 2011, Qingdao.

**Zhang J., Xie J.** Reservoir sedimentary facies // Beijing, Petroleum Industry Press, 2008.